

Local Optimization of Wave-fronts for high sensitivity PHase Imaging (LowPhi)

Thomas Juffmann,^{1,2,3} Andrs de los Ros Sommer,¹ and Sylvain Gigan¹

¹*Laboratoire Kastler Brossel, UPMC-Sorbonne Universits, ENS-PSL Research University, CNRS, Collge de France; 24 rue Lhomond, F-75005 Paris, France*

²*Faculty of Physics, University of Vienna, A-1090 Vienna, Austria*

³*Department of Structural and Computational Biology, Max F. Perutz Laboratories, University of Vienna, A-1030 Vienna, Austria*

Phase microscopy is an invaluable tool in the biosciences and in clinical diagnostics. The sensitivity of current phase microscopy techniques is optimized for one specific mean phase value and varies significantly across a given sample. Here, we demonstrate a technique based on wavefront shaping that optimizes the sensitivity across the field of view and for arbitrary phase objects. A significant mean sensitivity enhancement is achieved, both for engineered test samples, as well as for red blood cells. Besides sensitivity enhancement, the technique homogenizes sensitivity, reduces typical phase imaging artifacts such as halos, and allows for quantitative single-frame microscopy, which potentially allows for imaging speedup as compared to other phase stepping techniques.

I. INTRODUCTION

Phase microscopy [1] is an invaluable tool for the study of biological specimens such as cells, and has found both scientific and diagnostic applications [2, 3]. For flat samples the high sensitivity of phase microscopy allows for the detection of atomic steps on surfaces [4], and for the unlabeled detection of single proteins [5]. However, to date quantitative phase imaging of complex phase objects remains challenging, requiring either cumbersome setups or multiple frame acquisition. Wave-front shaping, the ability to digitally control the phase of incident light across large pixel arrays using MEMS or Liquid Crystal based technologies, has recently emerged as a powerful tool in microscopy and imaging. Various beam shaping techniques have been developed to enhance the capabilities of phase microscopes [6, 7], mostly by tailoring phase masks in the diffraction plane.

In interferometry, to determine the phase of a signal wave $E_S = |E_S|e^{i\phi}$, it has to be interfered with a reference wave $E_R = |E_R|e^{i\alpha}$. The resulting interference pattern reads $I = |E_S|^2 + |E_R|^2 \cos(\phi - \alpha)$, and its sensitivity to small changes of ϕ is proportional to $\sin(\phi - \alpha)$.

For measurements at optimal sensitivity α needs to be adjusted such that $\phi - \alpha = (2n-1)\pi/2$, with $|n| = 1, 2, 3, \dots$. At $\phi - \alpha = n\pi$ the sensitivity drops to zero.

In non-scanning phase microscopy, the interaction of a plane wave with a phase object causes local variations in its phase $E_S = |E_S|e^{i\phi(x,y)}$. For biological samples, such as cells, these spatial variations often cover the full range $(-\pi, \pi)$ and may even induce some phase wrapping. It is thus impossible to optimize the phase of a plane reference wave to achieve optimal sensitivity across the whole field of view. Here, we introduce a wave-front shaping technique that allows for high sensitivity full field phase imaging of samples that are not flat. We demonstrate how wave-front shaping can be used to restore optimal sensitivity across the whole field of view. We demonstrate the principle of our new technique in a standard phase contrast configuration, a common-path technique that is

intrinsically stable and widely used. We stress however, that LowPhi can also be applied to other phase imaging techniques, like holography, in which either the reference nor the signal beam can be appropriately shaped.

Zernike phase microscopy [1] is based on the insight that the optical field after sample interaction can be written as the sum of a plane (unscattered) reference wave and a scattered wave $E = |E|e^{i\psi(x,y)} = |E_R| + |E_S(x,y)|e^{i\phi(x,y)}$. In the Fourier plane (after propagation through a 2f setup), the reference wave is focused onto a point, while the scattered wave is spread out across the plane, which allows adding a phase α to the reference wave locally, without affecting the scattered wave:

$$E_F = |E_R|e^{i\alpha} + |E_S(x,y)|e^{i\phi(x,y)} \quad (1)$$

Propagation through another 2f setup yields an image of intensity

$$I(x,y) = |E_S(x,y)|^2 + |E_R|^2 \quad (2)$$

$$+ 2|E_S(x,y)||E_R| \cos(\phi(x,y) - \alpha) \quad (3)$$

For $\alpha = \pm\pi/2$, the conventional schemes of positive and negative phase contrast are retrieved, which represent optimal choices only if $\phi(x,y) \approx 0$.

Our technique (Fig. 1) uses a spatial light modulator to ensure this condition is met everywhere across the field of view of the image. First, a phase image of the sample is taken using a traditional quantitative phase imaging technique [8]. Then, a spatial light modulator (SLM) in a plane conjugate to the specimen plane (SP) is used to subtract the measured phase-shifts from the wave-front. This is in strong contrast with most techniques where the wavefront is controlled in the Fourier Plane. The resulting phase variations, $\psi(x,y) - \psi_{meas}(x,y)$ are given by the error of the first measurement, which can be due to statistical or systematic errors (e.g. due to imaging artifacts such as halo effects commonly observed in phase microscopy). If the error is non-negligible, the procedure can be applied iteratively until $\psi(x,y) - \psi_{meas}(x,y) \ll 1$ across the field of view. The choice of $\alpha = \pm\pi/2$ will now yield optimal sensitivity across the image. For dynamic

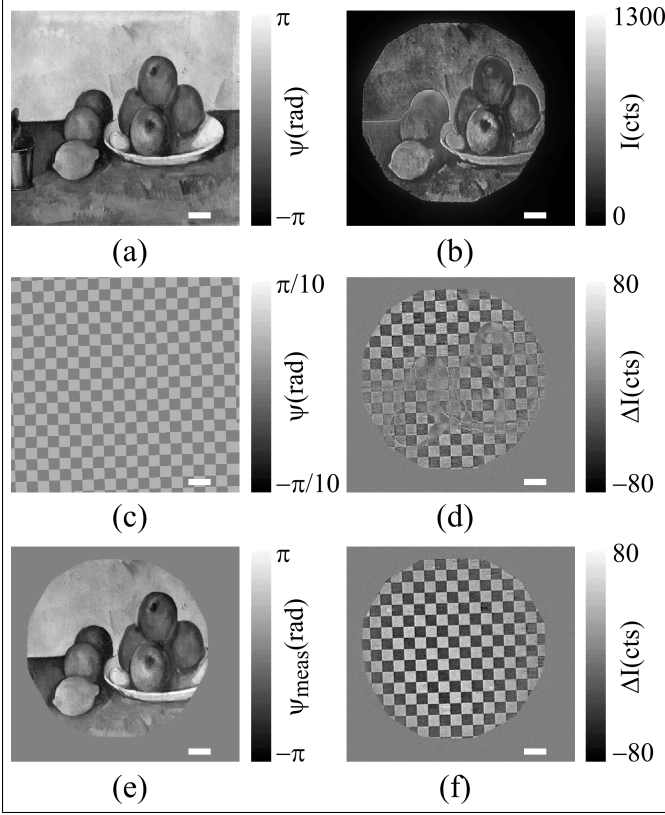


FIG. 2. (a) Cezanne's Still Life with Apples converted into a phase distribution (ψ_{CZ}). (b) negative phase contrast image of the phase distribution in (a). (c) Checkerboard phase distribution (ψ_{CB}) added to (a). (d) Acquiring a negative phase contrast image of $\psi = \psi_{CZ} + \psi_{CB}$ and subtracting it from the image in (b), reveals the intensity changes due to ψ_{CB} . (e) Iterative phase imaging and wavefront correction leads to an artifact free image of ψ_{CZ} . A negative phase contrast image of $\psi = \psi_{CZ} - \psi_{\text{meas}} + \psi_{CB}$ reveals the checkerboard with good signal-to-noise across the field of view. All scalebars are 400 microns.

(Fig. 2f), with good signal to noise and with a constant signal across the field of view.

IV. ANALYSIS

This observation is quantified in Fig. 3. The dashed (solid) green line in Fig. 3a shows a histogram of the background-subtracted, relative intensity changes due to the addition of the checkerboard phase distribution. The phase difference between the dark (dashed) and bright (solid) squares is $\psi_{CB} = 0.12$ rad, corresponding to a change of OPL of 10 nm. The unmodulated, incoherent background was measured by setting ψ_{CB} to $\pi/2$ and fitting the intensity of the dark squares with a fifth order polynomial. Note that it represents an additional term in (3) that does not affect the intensity of the interference term. The mean signal, e.g. the distance between the peaks of the dashed and the solid line, is increased for

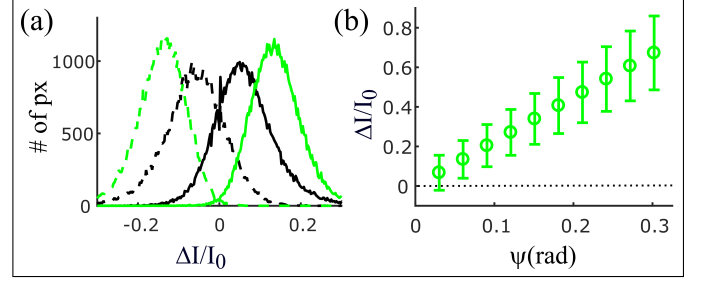


FIG. 3. (a) histogram of the relative intensity changes within the dark (dashed line) and bright (solid line) squares of the checkerboard, as measured via LowPhi (green) and phase contrast microscopy (black). (b) Distance of the peaks of the dashed and solid histograms as a function of the phase value added by the checkerboard. The error bars are obtained from error propagation, considering the widths of the histograms in (a).

LowPhi (green) as compared to negative phase contrast imaging (black), demonstrating the signal enhancing capabilities of LowPhi. Equally important is the reduction of the width of the two peaks (σ_{bright} and σ_{dark}) for LowPhi, which leads to negligible overlap of the two peaks, and increased signal to noise. This is not the case for negative phase contrast imaging, where significant overlap does not allow for a quantitative phase measurement.

LowPhi also yields a quantitative phase measurement. First, the SLM pattern provides a coarse estimate of the phase of the object. Then, if the SLM pattern is accurately compensating the object within less than a fraction of radian, the remaining phase shifts are small, $|E_S| \ll |E_R|$, and $|E_R| \approx |E|$. This yields $\Delta I(x, y)/I_0 \approx 2\psi(x, y)$, where $I_0 = |E_R|^2$, as can be derived by rewriting and squaring (1) as $|E_F|^2 = ||E_R|e^{i\alpha} + |E|e^{i\psi(x, y)} - |E_R||^2$. These conditions are fulfilled in LowPhi, allowing for single frame quantitative measurements. This is demonstrated in Fig. 3b, where the measured relative intensity changes in the background subtracted images are plotted as a function of ψ_{CB} , varying from 30 to 300 mrad (2.5 to 25 nm in OPL). For each value of ψ_{CB} , histograms analogous to those in Fig. 3a are calculated. The error bars σ in Fig. 3b denote the width of these histograms ($\sigma = \sqrt{\sigma_{\text{bright}}^2 + \sigma_{\text{dark}}^2}$). For the smallest phase shifts the width is dominated by statistics as evidenced by a 1.97x reduction in width when averaging four images. Future experiments will deploy higher intensity light sources and higher sensitivity detectors to enable increased sensitivity and higher frame rates. While in the current study phase noise on the SLM, which is typically highest at frequencies >50 Hz, was averaged out, this will not be the case in high frame rate studies. It might then be necessary to synchronize the light source to the SLM phase noise. For larger phase shifts, the width is currently dominated by spatial variations of the measured phase shifts. In future experiments, these can be reduced by a pixel-by-pixel calibration of the SLM and

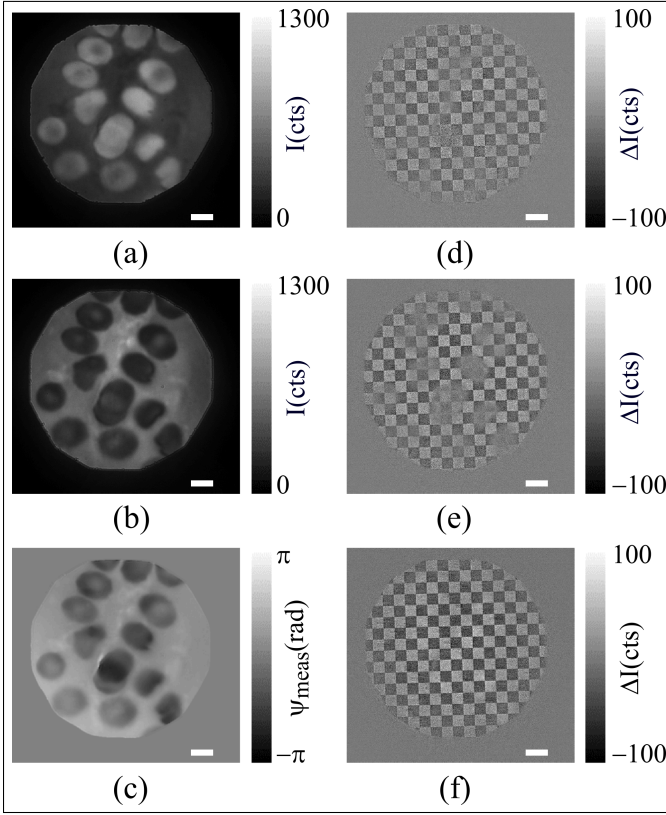


FIG. 4. Negative phase contrast, positive phase contrast and LowPhi images of red blood cells. Again, the local sensitivity to phase changes is probed by adding a checkerboard phase distribution, which is measured differentially as described in Fig.2. All scalebars are 8 microns.

by a better estimate and reduction of the unmodulated background light. Note that the finite step size of present day spatial light modulators does not pose a limit to the technique, as discretization can be considered in image analysis.

V. IMAGING OF BIOLOGICAL SPECIMENS

To test LowPhi under real imaging conditions, biological samples are introduced in the sample plane of the inverted phase microscope (see Fig. 1). A 50x objective is used to image them onto SLM1, which is used emulate the small phase shifts (checkerboard), as well as for LowPhi. Fig. 4a,b, and c show the images of red blood cells obtained in negative phase contrast, positive phase contrast, and LowPhi, respectively. The right column shows the respective results of differential checker-board measurements, where $\psi_{CB} = 0.12$ rad. Again, we see that the sensitivity is improved, more homogeneous, and quantitative using LowPhi.

VI. CONCLUSIONS AND OUTLOOK

LowPhi is a technique that uses wave-front shaping to optimize, and thus homogenize, the sensitivity of phase imaging across the field of view. Once initialized, LowPhi allows for high frame rate quantitative phase imaging without a phase-stepping algorithm. It minimizes imaging artifacts such as halo and shadow effects. We demonstrated these key advantages of LowPhi with both artificial and biological samples and showed significant local sensitivity enhancement. LowPhi is a common path technique and thus very stable. It can be set-up as an add-on to a conventional (inverted) phase contrast microscope. We stress however, that the principle can also be applied to techniques using an external reference wave, in which either the reference or the signal wave can be reshaped to guarantee optimal sensitivity. Besides high speed quantitative studies of cell dynamics and morphology, LowPhi may also find use in multi-pass microscopy [10, 11] to avoid phase wrapping problems. To achieve this, an SLM would have to be incorporated within the self-imaging cavity of a multi-pass microscope, again in a plane that is conjugate to the sample. Considering recent advances in electron optics [12, 13], LowPhi might also be interesting for electron microscopy, where, due to specimen damage, it is absolutely crucial to achieve highest sensitivity per electron-sample interaction [14].

FUNDING INFORMATION

HFSP Cross-Disciplinary Fellowship (LT000345/2016-C); ERC SMARTIES (Grant 724473)

ACKNOWLEDGMENTS

The authors thank J. Dong for helpful discussions.

SUPPLEMENTAL INFORMATION

Figure 5 shows the LowPhi configuration that was used in the experiment. It enables LowPhi as an add-on to a commercial inverted microscope. A single reflective SLM is used to modulate the wave-front in a plane conjugate to the sample as well as in the Fourier plane.

First, a wavefront coming from a commercial microscope is in-coupled using a beamsplitter (BS1) and imaged onto the left half of the SLM, which is conjugate to the sample. Then, a folded 2f system is used to propagate the wavefront to the right half of the SLM, where the wavefront can be modulated in Fourier space. A second beam splitter (BS2) is used to direct the remaining fraction of the wavefront to a CMOS detector. To minimize reflections back and forth between the two planes, BS1 was chosen to have a 90 to 10 ratio of reflected to transmitted intensity. A knife-edge right-angle prism mirror

- FIG. 5. Folded LowPhi configuration (see text).